Developments on the holographic superconductor and superfluid with excited states

Qiyuan Pan

湖南師範大學 HUNAN NORMAL UNIVERSITY

Based on works: *JHEP* 12, 192 (2020); *PLB* 811, 135864 (2020); *PLB* 823, 136755 (2021); *SCPMA* 64, 240411 (2021); *PLB* 845, 138134 (2023); *NPB* 991, 116223 (2023); *PRD* 110, 046003 (2024)

2025年7月18日

Outline:

1. **Introduction**
2. **Holographic superconductor with excited states**
3. **Holographic superfluid with excited states**
4. **Conclusions**

1、 Introduction

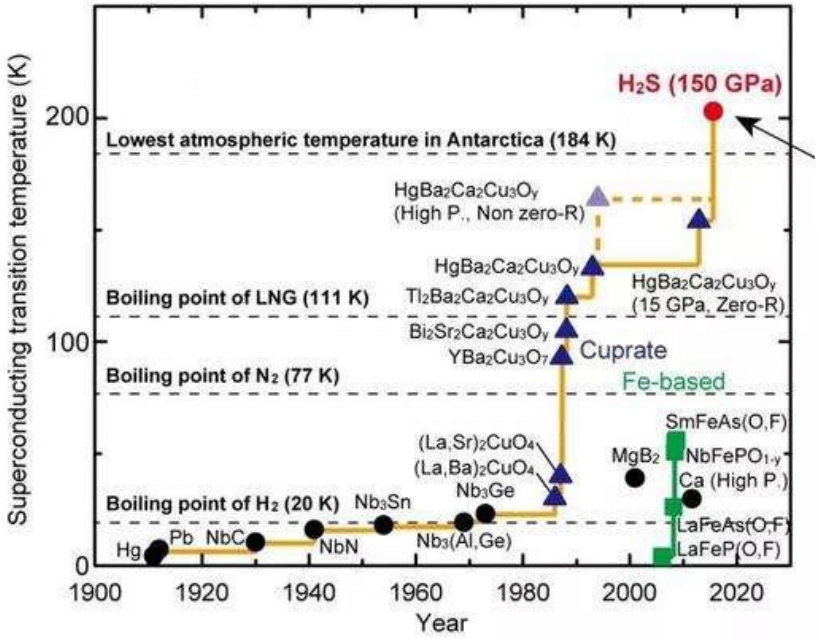

硫化氢创下超导临界温度最高纪录--科技--人民网

2015年8月20日 - ,德国科学家在新一期学术期刊《自然》上报告说,他们发现在150万巴(约合148万个标准大气压)的压强下,硫化氢可在零下70摄氏度的"高温"下呈现超导性...

scitech.people.com.cn/... - 百度快照

人类逼近物理"圣杯":-23℃超导!德国科学家再次突破高温超导纪录

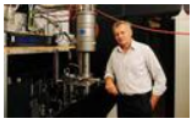

2018年12月20日 - -23℃ 实现超导,人类高温超导记录被刷新。该突破由德国马普化学研究所的 Mikhail Eremets 与其同事带来,他们在250K (-23℃)温度下实现了 LaH...

观察者网 - 百度快照

LaH10 （氢化镧 ）

In modern condensed matter physics, one of the unsolved mysteries is the core mechanism governing the high-temperature superconductors which are not described by the usual Bardeen-Cooper-Schrieffer (BCS) theory.

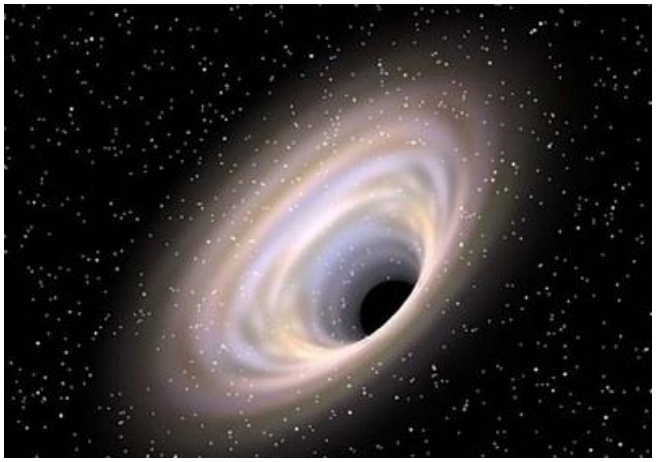

Black hole

High T_c superconductor

a gravity theory in a n-dimensional anti-de Sitter (AdS) spacetime

AdS/CFT correspondence

a conformal field theory on the (n-1)-dimensional boundary of AdS

Gravity	Superconductor
Black hole	Temperature
Charged scalar field	Condensate

Need to find a black hole which has scalar hair at low temperatures, but no hair at high temperatures! ------How to find…?

Gubser (08) consider the action with a Maxwell field and a charged complex scalar field:

S.S. Gubser, *PRD* 78, 065034 (2008)

$$\mathcal{L} = \frac{1}{2\kappa^2}\left[R - \frac{1}{4}F_{\mu\nu}^2 - |(\partial_\mu - iqA_\mu)\psi|^2 + \frac{6}{L^2} - m^2|\psi|^2\right]$$

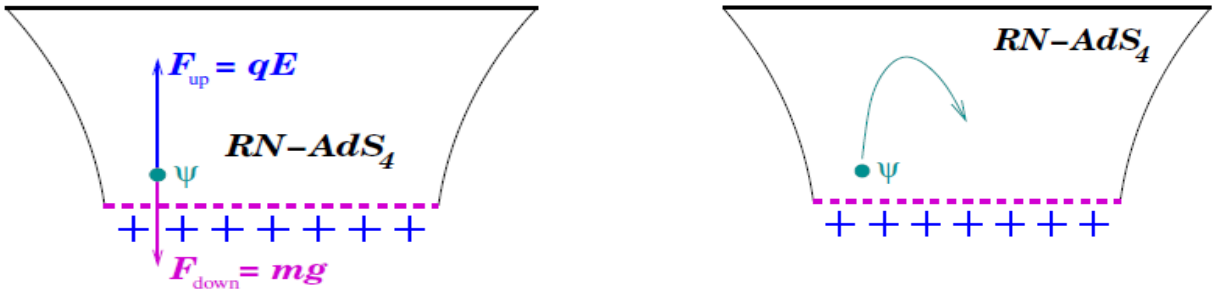

the emergence of the scalar hair in the bulk AdS black hole

the formation of a charged condensation in the boundary dual CFTs

Holographic *s*-wave superconductor in the probe limit

Hartnoll et al. *PRL* 101, 031601 (2008)

A Maxwell field and a charged complex scalar field with Lagrangian density:

$$\mathcal{L} = -\frac{1}{4}F^{ab}F_{ab} - V(|\Psi|) - |\partial\Psi - iA\Psi|^2$$

The potential: $$V(|\Psi|) = -\frac{2|\Psi|^2}{L^2}$$

The planar Schwarzschild–anti-de Sitter black hole:

$$ds^2 = -f(r)dt^2 + \frac{dr^2}{f(r)} + r^2(dx^2 + dy^2)$$

The metric function: $$f = \frac{r^2}{l^2} - \frac{M}{r}$$

The equation of motion:

$$\Psi'' + \left(\frac{f'}{f} + \frac{2}{r}\right)\Psi' + \frac{\Phi^2}{f^2}\Psi + \frac{2}{L^2 f}\Psi = 0$$

$$\Phi'' + \frac{2}{r}\Phi' - \frac{2\Psi^2}{f}\Phi = 0$$

Properties of the dual field theory can be read off from the asymptotic behavior of the solution

Integrating out to infinity, these solutions behave as

$$\Psi = \frac{\Psi^{(1)}}{r} + \frac{\Psi^{(2)}}{r^2} + \cdots$$

$$\Phi = \mu - \frac{\rho}{r} + \cdots$$

μ: chemical potential ; ρ: charge density

The condensate of the scalar operator $\mathcal{O}$ in the field theory dual to the field Ψ is given by

$$\langle \mathcal{O}_i \rangle = \sqrt{2}\Psi^{(i)}\,, \quad i = 1, 2$$

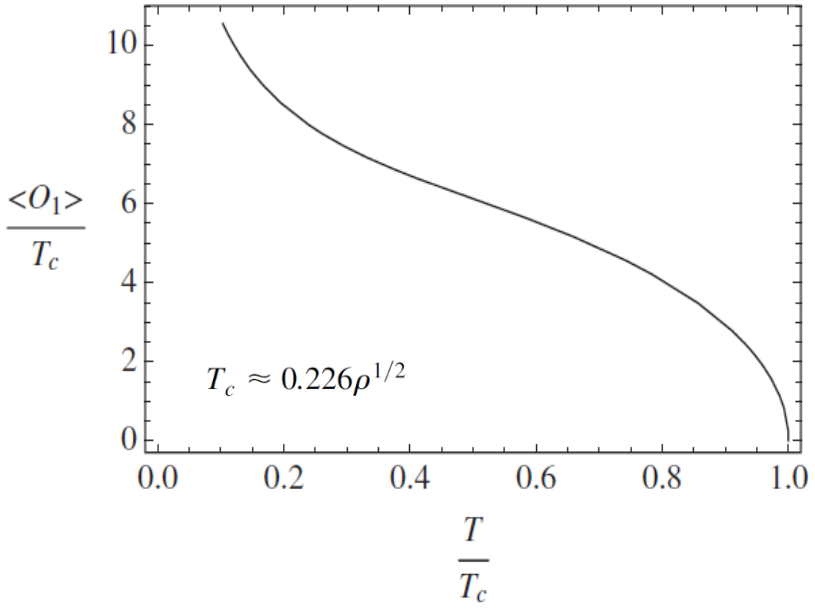

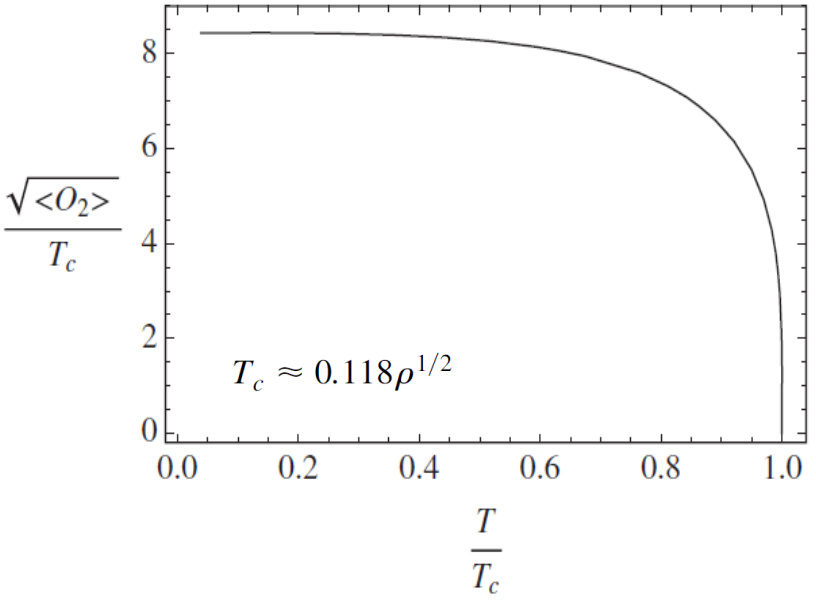

$$\langle \mathcal{O}_1 \rangle \approx 9.3\, T_c\, (1 - T/T_c)^{1/2}\,, \qquad T \to T_c$$

$$\langle \mathcal{O}_2 \rangle \approx 144\, T_c^2\, (1 - T/T_c)^{1/2}\,, \quad T \to T_c$$

It is expected that this condensate will lead to superconductivity

Conductivity of holographic superconductors with various condensates

Horowitz et al. *PRD* 78, 126008 (2008)

To compute the conductivity in the dual CFT, the perturbations of the vector potential were considered

$$A_x'' + \left(\frac{f'}{f} + \frac{d-3}{r}\right)A_x' + \left(\frac{\omega^2}{f^2} - \frac{k^2}{r^2 f} - \frac{2\psi^2}{f}\right)A_x = 0.$$

For the case of d=3:

Asymptotic behavior: $A_x = A^{(0)} + \frac{A^{(1)}}{r} + \cdots$

Conductivity: $\sigma(\omega) = \frac{1}{i\omega} G^R(\omega, k=0) = \frac{A^{(1)}}{i\omega A^{(0)}}\Big|_{k=0}$

For the case of d=4:

Asymptotic behavior: $A_x = A^{(0)} + \frac{A^{(2)}}{r^2} + \frac{A^{(0)}(\omega^2 - k^2)}{2}\frac{\log \Lambda r}{r^2}\cdots$

Conductivity: $\sigma = \frac{2A^{(2)}}{i\omega A^{(0)}}\Big|_{k=0} + \frac{i\omega}{2}$

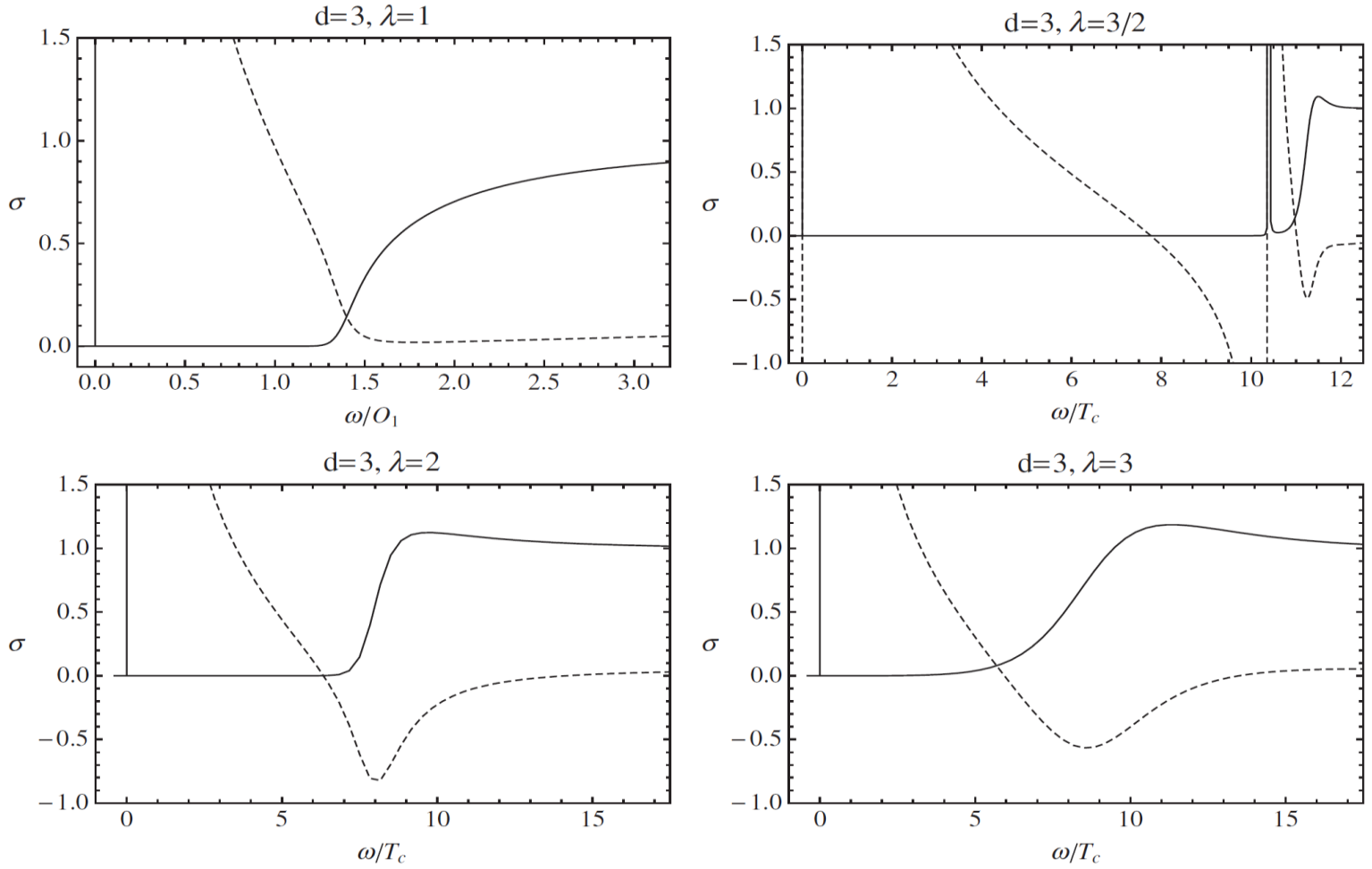

For the case of d=3: the solid line is the real part and dashed is imaginary

For all cases with $\lambda > \lambda_{\mathrm{BF}}$, we find

$$\frac{\omega_g}{T_c} \approx 8$$

ω_g : the gap frequency;

λ_{BF} : corresponds to the case of lower bound called the Breitenlohner-Freedman (BF) bound for the scalar mass

A robust feature: Since the corresponding BCS value is 3.5, this shows that the energy to break apart the condensate is more than twice the weakly coupled value

Holographic superconductors with various condensates in Einstein-Gauss-Bonnet gravity

Gregory, Kanno and Soda, *JHEP* 10, 010 (2009)

Pan, Wang, et al. *PRD* 81, 106007 (2010)

Influences of the $1/N$ or $1/\lambda$ (λ is the 't Hooft coupling) corrections on the holographic dual models

The model:

$$\mathcal{L}_{R^2} = \tilde{\alpha}\left(R_{\mu\nu\gamma\delta}R^{\mu\nu\gamma\delta} - 4R_{\mu\nu}R^{\mu\nu} + R^2\right)$$

$$S = \int d^dx\sqrt{-g}\left\{\frac{1}{16\pi G}\left[R + \frac{(d-1)(d-2)}{L^2} + \mathcal{L}_{R^2}\right] + \left(-\frac{1}{4}F_{\mu\nu}F^{\mu\nu} - |\nabla\psi - iA\psi|^2 - m^2|\psi|^2\right)\right\}$$

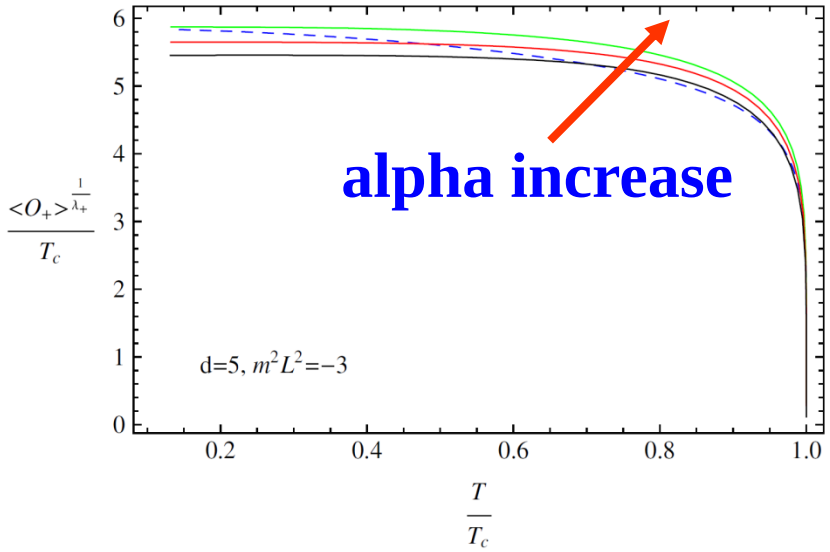

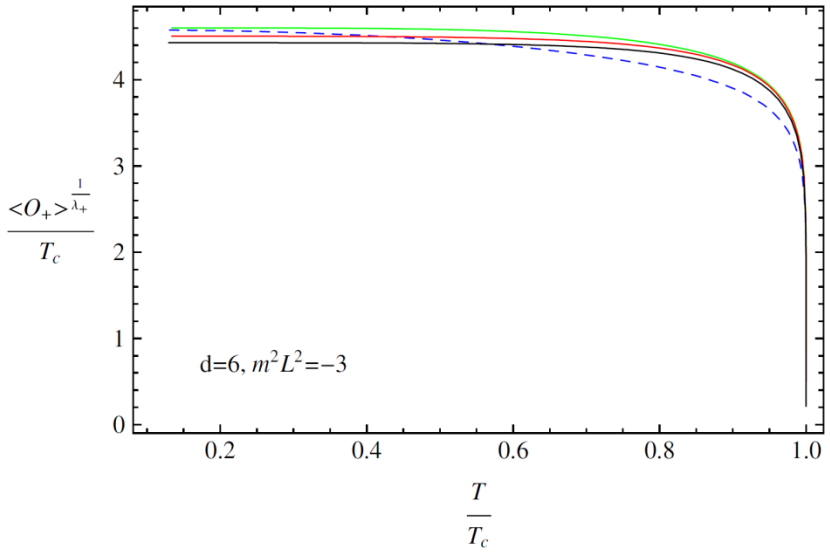

Higher order curvature corrections make the condensation harder to form

Holographic superconductor models with the Maxwell field strength corrections

Pan*, Jing and Wang, *PRD* 84, 126020 (2011)

The model:

$$\mathcal{L}_{F^4} = c_1 (F_{\mu\nu}F^{\mu\nu})^2 + c_2 F_{\mu\nu}F^{\nu\delta}F_{\delta\kappa}F^{\kappa\mu}$$

$$S = \int d^d x \sqrt{-g} \left(-\frac{1}{4} F_{\mu\nu}F^{\mu\nu} + \mathcal{L}_{F^4} - |\nabla\psi - iA\psi|^2 - m^2|\psi|^2 \right)$$

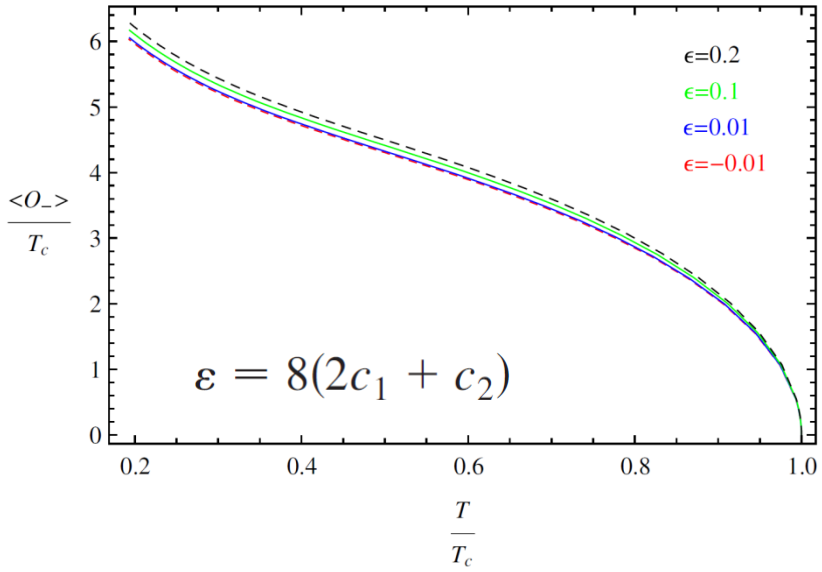

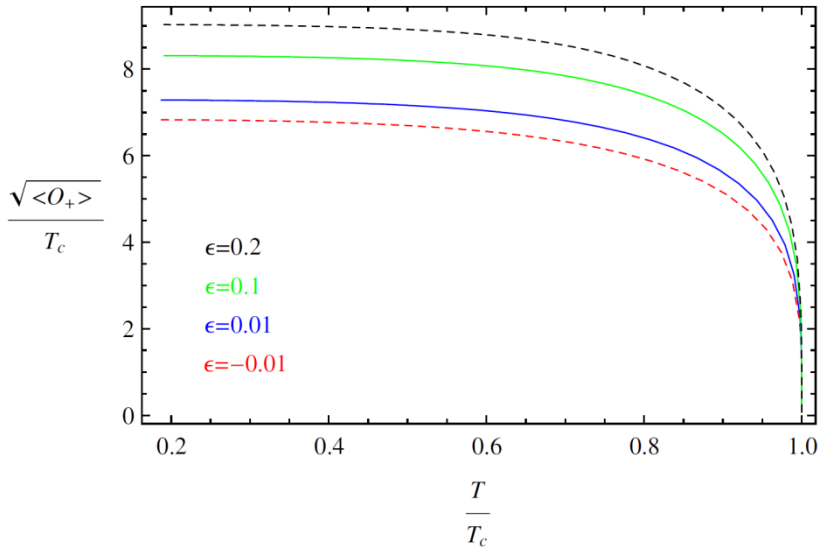

The scalar hair is harder to be formed when adding the corrections to the usual Maxwell field. This effect is similar to that caused by the curvature correction.

Motivation: All the studies mentioned above concerning the holographic superconductors are mainly based on the ground state since it is the first state to condense

(a) In condensed matter physics, the physical system is not necessarily in equilibrium, but may remain the excited metastable states

G.F. Zharkov, *Phys. Rev. B* 63 (2001)

(b) For the mesoscopic nanomaterials, the thermal fluctuation of the system may make it turn into metastable states and the system may remain in these states for a long time

F. Peeters, V. Schweigert, B. Baelus and P. Deo, *Physica C* 332, 255 (2000)

(c) For the nanowires, the potential of superconducting nanowires lies in their long-lived excited states

J.E. Mooij and C.J.P. Harmans, *New J. Phys.* 7 (2005) 219

2. Holographic superconductors with excited states

2.1 Holographic s-wave superconductor with excited states (in the Einstein gravity)

Wang, Hu, Liu, Yang and Zhao, *JHEP* 06, 013 (2020)

The action:

$$\mathcal{S}=\frac{1}{16\pi G}\int \mathrm{d}^4x\left[R+\frac{6}{\ell^2}-\frac{1}{4}F^{\mu\nu}F_{\mu\nu}-(\mathcal{D}_\mu\psi)(\mathcal{D}^\mu\psi)^*-m^2\psi\psi^*\right]$$

In the probe limit, the metric:

$$f(r)=\frac{r^2}{\ell^2}(1-r_h^3/r^3)$$

$$ds^2=-f(r)dt^2+\frac{dr^2}{f(r)}+r^2(dx^2+dy^2)$$

The equation of motion:

$$A=\phi(r)dt\,,\qquad \psi=\psi(r)$$

$$\psi''+\left(\frac{f'}{f}+\frac{2}{r}\right)\psi'+\frac{\phi^2}{f^2}\psi-\frac{m^2}{\ell^2 f}\psi=0\,,$$

$$\phi''+\frac{2}{r}\phi'-\frac{2\psi^2}{f}\phi=0.$$

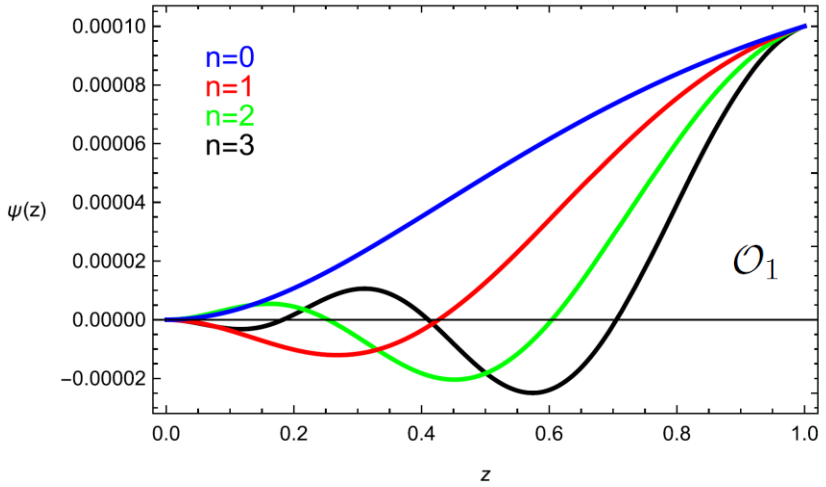
n=0
n=1
n=2
n=3
ψ(z)
z
$\mathcal{O}_1$

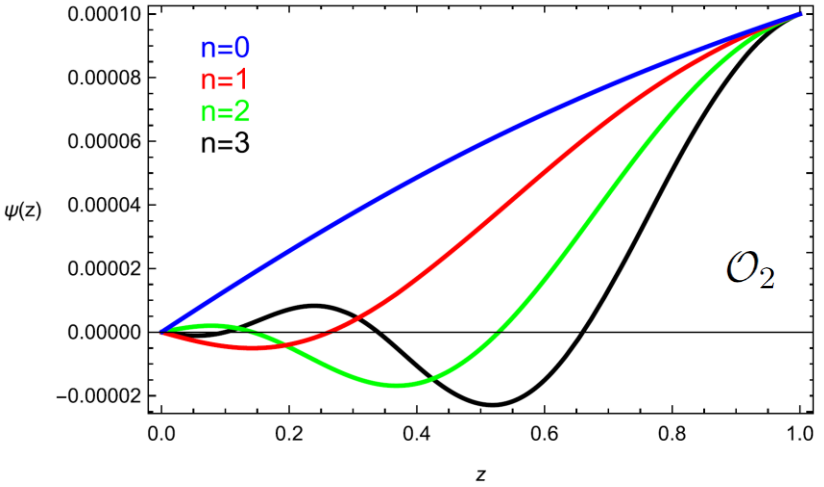
n=0
n=1
n=2
n=3
ψ(z)
z
$\mathcal{O}_2$

$$m^2 = -2$$

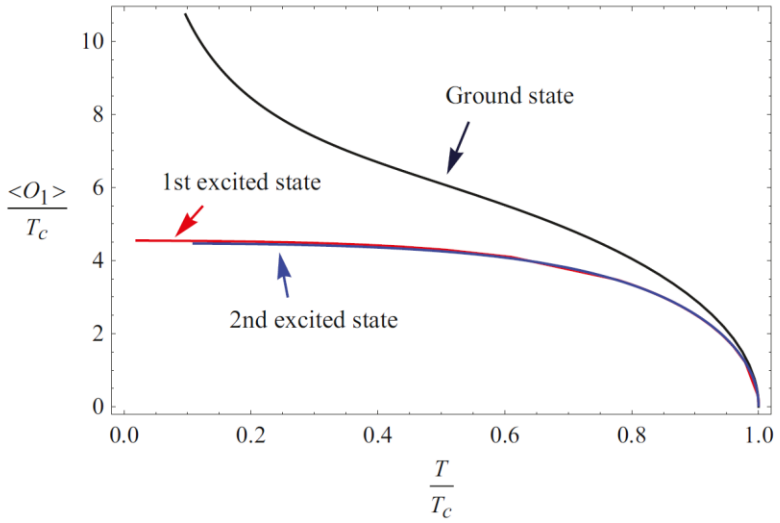
Ground state
1st excited state
2nd excited state
$\frac{<O_1>}{T_c}$
$\frac{T}{T_c}$

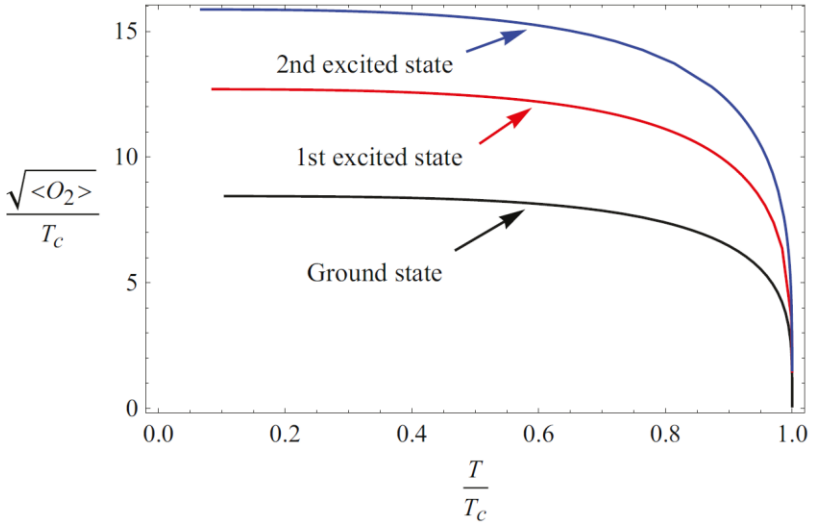
2nd excited state
1st excited state
Ground state
$\frac{\sqrt{<O_2>}}{T_c}$
$\frac{T}{T_c}$

$$\langle \mathcal{O}_1 \rangle \approx \begin{cases} 9.3\, T_c^{(0)} (1 - T/T_c^{(0)})^{1/2}, & \text{Ground state,} \\ 8.9\, T_c^{(1)} (1 - T/T_c^{(1)})^{1/2}, & \text{1st excited state,} \\ 8.5\, T_c^{(2)} (1 - T/T_c^{(2)})^{1/2}, & \text{2nd excited state.} \end{cases}$$

where the critical temperatures $T_c^{(0)} \approx 0.226\rho^{1/2}$, $T_c^{(1)} \approx 0.094\rho^{1/2}$ and $T_c^{(2)} \approx 0.07\rho^{1/2}$, correspond to the ground, first and second excited states, respectively.

$$\langle \mathcal{O}_2 \rangle \approx \begin{cases} 144\, (T_c^{(0)})^2 (1 - T/T_c^{(0)})^{1/2}, & \text{Ground state,} \\ 329\, (T_c^{(1)})^2 (1 - T/T_c^{(1)})^{1/2}, & \text{1st excited state,} \\ 512\, (T_c^{(2)})^2 (1 - T/T_c^{(2)})^{1/2}, & \text{2nd excited state.} \end{cases}$$

where $T_c^{(0)} \approx 0.118\rho^{1/2}$, $T_c^{(1)} \approx 0.079\rho^{1/2}$ and $T_c^{(2)} \approx 0.063\rho^{1/2}$ correspond to the ground, first and second excited states, respectively.

(1) The phase transition of the holographic s-wave superconductors with excited states belongs to the second order with the critical exponent 1/2.

(2) The excited state has a lower critical temperature than the corresponding ground state, indicating that the higher excited state makes the scalar condensate harder to form.

The critical chemical potential

μ_c \ n	0	1	2	3	4	5	6
$\langle \mathcal{O}_1 \rangle$	1.120	6.494	11.701	16.898	22.094	27.290	32.486
$\langle \mathcal{O}_2 \rangle$	4.064	9.188	14.357	19.538	24.725	29.915	35.107

Table 1. Critical chemical potential μ_c for the operators $\mathcal{O}_1$ and $\mathcal{O}_2$ from the ground state to sixth excited state.

$$\mu_c \approx \begin{cases} 5.217n + 1.217\,, & \text{for } \mathcal{O}_1\,, \\ 5.177n + 4.026\,, & \text{for } \mathcal{O}_2\,. \end{cases}$$

The difference of the dimensionless critical chemical potential between the consecutive states is around 5

Conductivity of holographic superconductors with excited states

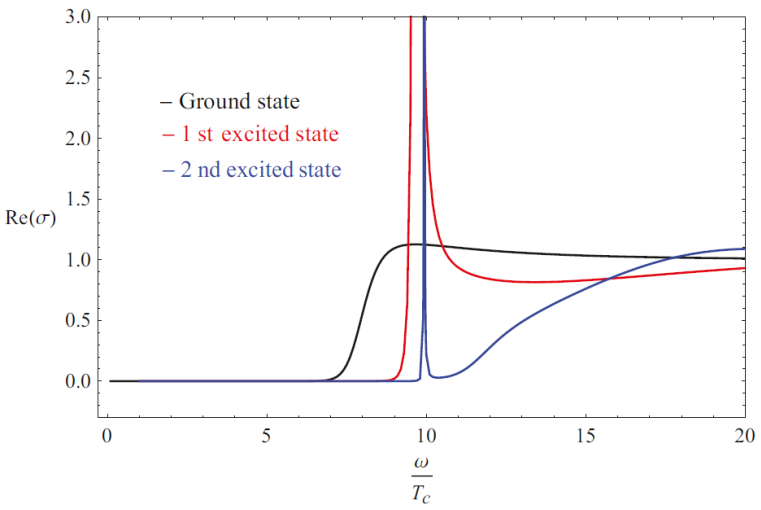

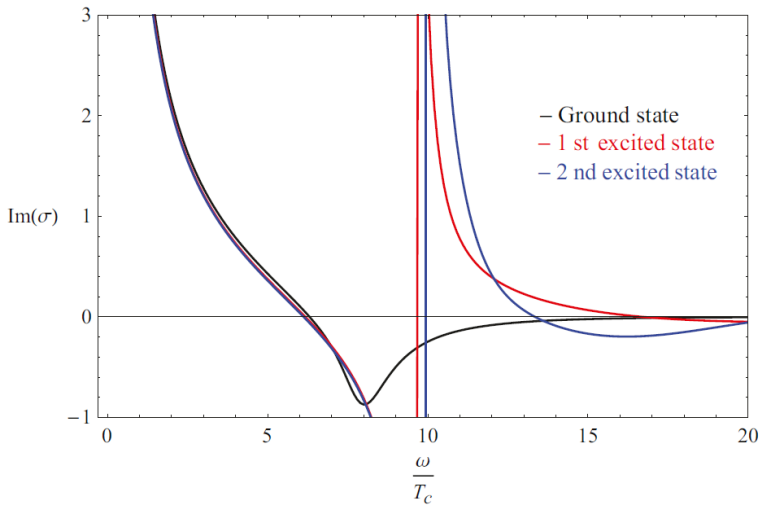

The conductivity of each excited state has an additional pole in the imaginary part of the conductivity and a delta function in the real part arising at the low temperature inside the gap, which is just the evidence of the existence of excited states.

2.2 An analytic study on excited states of holographic superconductors

Qiao, Wang, OuYang, Wang*, **Pan*** and Jing, *PLB* 811, 135864 (2020)

OuYang, Wang, Qiao, Wang, **Pan*** and Jing, *SCPMA* 64, 240411 (2021)

Sturm-Liouville (S-L) problem

Euler equation：
$$\frac{d}{dx}\left(p(x)\frac{dy(x)}{dx}\right)+q(x)y(x)+\lambda r(x)y(x)=0$$

the following boundary conditions:

$$(p(x)y'(x))|_{x=a}=0 \quad or \quad y(a)\ prescribed$$
$$(p(x)y'(x))|_{x=b}=0 \quad or \quad y(b)\ prescribed.$$

the determination of stationary values of the quantity λ defined by the ratio

$$\lambda=\frac{\int_a^b\left\{p(x)(y'(x))^2-q(x)y^2(x)\right\}dx}{\int_a^b r(x)y^2(x)dx}$$

The equations of the motion for the z coordinate:

$$\psi'' + \frac{f'}{f}\psi' - \frac{1}{z^4}\left[\frac{m^2}{f} - \frac{1}{f^2}\left(\frac{\phi}{r_+}\right)^2\right]\psi = 0\,,$$

$$\phi'' - \frac{2\psi^2}{z^4 f}\phi = 0,$$

$$f = (1/z^2 - z)/L^2$$

and below the critical point:

$$\phi(z) = \mu(1-z) = \lambda r_{+c}(1-z)$$

According to the asymptotical behavior of the scalar field, we take

$$\psi(z) \sim \frac{\langle O_i \rangle}{\sqrt{2} r_+^{\Delta_i}} z^{\Delta_i} F(z) \qquad F(0) = 1$$

which leads to

$$(TF')' + T\left[U + V\left(\frac{\mu}{r_+}\right)^2\right]F = 0$$

$$T(z) = \frac{z^{2(\Delta_i - 1)}(1-z^3)}{L^2}\,, \qquad U(z) = \frac{\Delta_i}{z}\left(\frac{\Delta_i - 1}{z} + \frac{f'}{f}\right) - \frac{m^2}{z^4 f}\,, \qquad V(z) = \frac{(1-z)^2}{z^4 f^2}$$

By making use of the Sturm-Liouville approach, we have

$$\left(\frac{\mu}{r_+}\right)^2 = \lambda^2 = \frac{\int_0^1 T\left(F'^2 - UF^2\right)dz}{\int_0^1 TVF^2 dz}$$

Including the ninth order of z in the trial function

$F(z) = 1 - \sum_{k=2}^{k=9} a_k z^k$ for the operator O_1, and $F(z) = 1 - \sum_{k=1}^{k=9} a_k z^k$ for the operator O_2

[25]: *JHEP* 06, 013 (2020)

Table 1

The dimensionless critical chemical potential μ_c/r_+ for the operator O_1 and corresponding value of a_k for the trial function $F(z) = 1 - \sum_{k=2}^{k=9} a_k z^k$ in the holographic s-wave superconductor. The results of μ_c/r_+ are obtained analytically by the Sturm-Liouville method (left column) and numerically by the spectral method [25] (right column) from the ground state to the fifth excited state.

n	μ_c/r_+		a_2	a_3	a_4	a_5	a_6	a_7	a_8	a_9
0	1.120	1.120	0.628	-0.584	0.031	0.507	-0.636	0.412	-0.148	0.023
1	6.493	6.494	21.006	-12.433	-87.517	217.020	-242.872	150.734	-49.962	6.827
2	11.700	11.701	66.377	7.206	-1310.093	4208.241	-6279.568	5139.829	-2245.136	411.703
3	16.901	16.898	142.425	29.025	-5888.970	25509.602	-49071.741	49823.574	-26164.029	5624.096
4	22.258	22.094	370.979	-2616.084	3486.249	15827.106	-61194.858	85570.988	-55240.956	13794.571
5	28.055	27.290	804.021	-10643.884	57037.950	-159446.972	252736.492	-229055.289	110764.290	-22192.871

By including more higher order terms in the expansion of the trial function, we observe that the analytic results agree well with the numeric data, which indicates that the Sturm-Liouville method is very powerful to study the holographic superconductors even if we consider the excited states.

The **analytical** critical chemical potential

$$\frac{\mu_c}{r_+} \approx \begin{cases} 5.347n + 1.053\,, & \text{for } O_1 \\ 5.322n + 3.840\,, & \text{for } O_2 \end{cases}$$

For the operator

$$\langle O_1 \rangle \approx \begin{cases} 8.2T_c^{(0)}(1 - T/T_c^{(0)})^{1/2}\,, & \text{the ground state with } T_c^{(0)} \approx 0.226\rho^{1/2}\,, \\ 6.6T_c^{(1)}(1 - T/T_c^{(1)})^{1/2}\,, & \text{the 1st excited state with } T_c^{(1)} \approx 0.094\rho^{1/2}\,, \\ 6.2T_c^{(2)}(1 - T/T_c^{(2)})^{1/2}\,, & \text{the 2nd excited state with } T_c^{(2)} \approx 0.070\rho^{1/2}\,, \end{cases}$$

$$\langle O_2 \rangle \approx \begin{cases} 119(T_c^{(0)})^2(1 - T/T_c^{(0)})^{1/2}\,, & \text{the ground state with } T_c^{(0)} \approx 0.118\rho^{1/2}\,, \\ 245(T_c^{(1)})^2(1 - T/T_c^{(1)})^{1/2}\,, & \text{the 1st excited state with } T_c^{(1)} \approx 0.079\rho^{1/2}\,, \\ 364(T_c^{(2)})^2(1 - T/T_c^{(2)})^{1/2}\,, & \text{the 2nd excited state with } T_c^{(2)} \approx 0.063\rho^{1/2} \end{cases}$$

Both of them agree well with the numerical data obtained by the spectral method in *JHEP* 06, 013 (2020).

2.3 Holographic entanglement entropy and subregion complexity for excited states of holographic superconductors (in the Einstein gravity and 4D Gauss-Bonnet gravity)

Wang, Qiao, Wang*, **Pan*,** Lai* and Jing, *NPB* 991, 116223 (2023)

Qiao, OuYang, Wang, **Pan*** and Jing, *JHEP* 12, 192 (2020)

Pan, Qiao, Wang, **Pan*,** Nie* and Jing*, *PLB* 823, 136755 (2021)

The action: $$S = \int dtd^3xN\sqrt{\gamma}\left(\mathcal{L}^{\rm 4D}_{\rm EGB} - \frac{1}{4}F_{\mu\nu}F^{\mu\nu} - |\nabla\psi - iqA\psi|^2 - m^2|\psi|^2\right)$$

$$\mathcal{L}^{\rm 4D}_{\rm EGB} = \frac{1}{2\kappa^2}\left\{2R + \frac{6}{L^2} - \mathcal{M} + \frac{\alpha}{2}\left[8R^2 - 4R\mathcal{M} - \mathcal{M}^2 - \frac{8}{3}\left(8R_{ij}R^{ij} - 4R_{ij}\mathcal{M}^{ij} - \mathcal{M}_{ij}\mathcal{M}^{ij}\right)\right]\right\}$$

Aoki, Gorji and Mukohyama, *PLB* 810 (2020) 135843; arXiv:2005.03859 [gr-qc]

The metric ansatz: $ds^2 = g_{\mu\nu}dx^\mu dx^\nu = -N^2dt^2 + \gamma_{ij}(dx^i + N^idt)(dx^j + N^jdt)$

$$N = \sqrt{f(r)}e^{-\chi(r)/2}\,, \qquad N^i = 0\,, \qquad \gamma_{ij} = {\rm diag}\left(\frac{1}{f(r)}, r^2, r^2\right)$$

The equations of motion: $A = \phi(r)dt\,, \qquad \psi = \psi(r)$

$$\psi'' + \left(\frac{2}{r} - \frac{\chi'}{2} + \frac{f'}{f}\right)\psi' + \left(\frac{q^2 e^{\chi}\phi^2}{f^2} - \frac{m^2}{f}\right)\psi = 0,$$

$$\phi'' + \left(\frac{2}{r} + \frac{\chi'}{2}\right)\phi' - \frac{2q^2\psi^2}{f}\phi = 0,$$

$$f' - \frac{1}{r^2 - 2\alpha f}\left(\frac{3r^3}{L^2} - rf - \frac{\alpha f^2}{r}\right) + \frac{\kappa^2 r^3}{r^2 - 2\alpha f}\left[m^2\psi^2 + \frac{1}{2}e^{\chi}\phi'^2 + f\left(\psi'^2 + \frac{q^2 e^{\chi}\phi^2\psi^2}{f^2}\right)\right] = 0,$$

$$\chi' + \frac{2\kappa^2 r^3}{r^2 - 2\alpha f}\left(\psi'^2 + \frac{q^2 e^{\chi}\phi^2\psi^2}{f^2}\right) = 0,$$

The asymptotic expressions near the boundary

$$\chi \to 0, \quad f \sim \frac{r^2}{L_{eff}^2}, \quad \phi \sim \mu - \frac{\rho}{r}, \quad \psi \sim \frac{\psi_-}{r^{\lambda_-}} + \frac{\psi_+}{r^{\lambda_+}}$$

$$L_{eff}^2 = \frac{2\alpha}{1 - \sqrt{1 - \frac{4\alpha}{L^2}}}, \qquad \lambda_\pm = (3 \pm \sqrt{9 + 4m^2 L_{eff}^2})/2$$

Condensates of the scalar field (the Einstein gravity as an example)

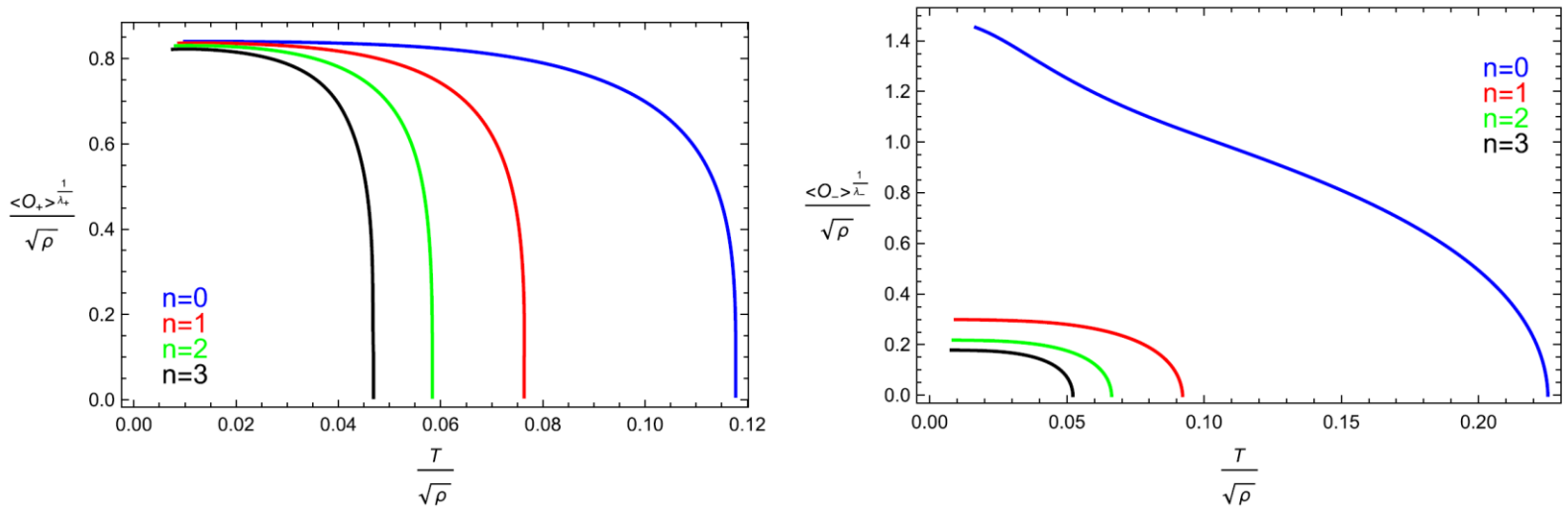

Fig. 2. The condensates of scalar operators $\mathcal{O}_+$ (left) and $\mathcal{O}_-$ (right) with excited states versus temperature for the fixed mass $m^2L^2 = -2$. In each panel, the blue, red, green and black lines denote the ground ($n = 0$), first ($n = 1$), second ($n = 2$) and third ($n = 3$) states, respectively.

Table 1
The critical temperature T_c of scalar operators $\mathcal{O}_+$ and $\mathcal{O}_-$ with excited states for the fixed mass $m^2L^2 = -2$. $q = 1 \;\; \kappa = 0.05$

n	0	1	2	3	4
$<\mathcal{O}_+>$	$0.117710\rho^{1/2}$	$0.076345\rho^{1/2}$	$0.058377\rho^{1/2}$	$0.046861\rho^{1/2}$	$0.038202\rho^{1/2}$
$<\mathcal{O}_->$	$0.225271\rho^{1/2}$	$0.092168\rho^{1/2}$	$0.066290\rho^{1/2}$	$0.052181\rho^{1/2}$	$0.042283\rho^{1/2}$

Holographic entanglement entropy and subregion complexity

Consider a subsystem A with a straight strip geometry

$$-l/2 \leq x \leq l/2 \ \text{ and } -R/2 \leq y \leq R/2 \ (R \to \infty)$$

with l: the size of region A, and R: a regulator which will be set to infinity

The induced metric on the minimal surface:

$$ds^2_{induced} = \frac{r_+^2}{z^2}\left\{\left[1 + \frac{1}{z^2 f}\left(\frac{dz}{dx}\right)^2\right]dx^2 + dy^2\right\}$$

The holographic entanglement entropy (HEE):

$$\mathcal{S} = \frac{R}{2G_4}\int_\epsilon^{z_\epsilon} \frac{z_*^2}{z^3\sqrt{(z_*^4 - z^4)f}}dz = \frac{R}{2G_4}\left(s + \frac{1}{\epsilon}\right)$$

a UV cutoff ϵ

The holographic subregion complexity (HSC):

$$\mathcal{C} = \frac{R}{4\pi L G_4}\int_\epsilon^{z_*} \frac{x(z)dz}{z^4 f} = \frac{R}{4\pi L G_4}\left[c + \frac{F(z_*)}{\epsilon^2}\right]$$

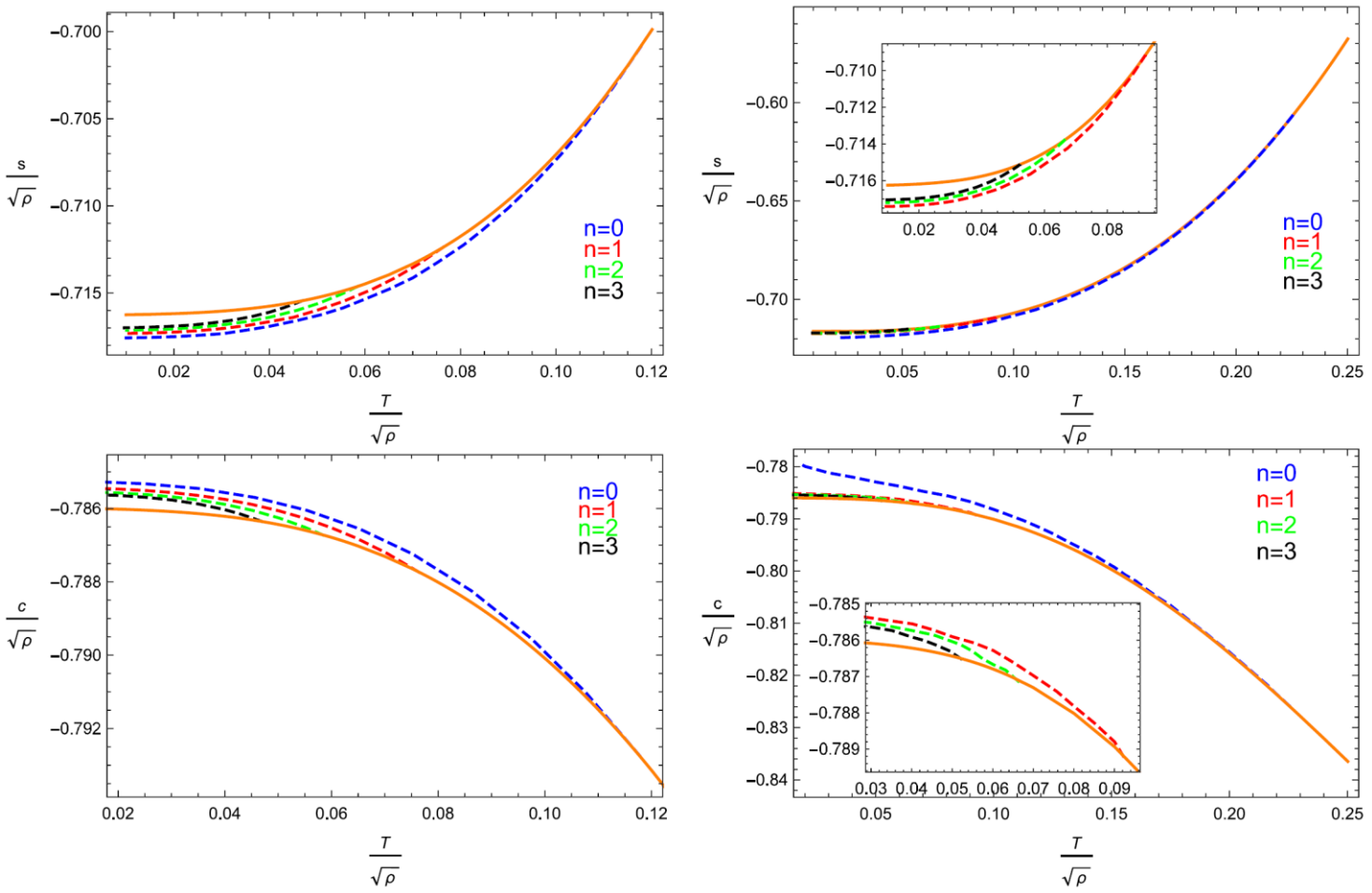

The values of T_c reflected by the holographic entanglement entropy (HEE) and holographic subregion complexity (HSC) are consistent with the results obtained from the condensate behavior, which means that both the HEE and HSC can be utilized as good probes to the superconducting phase transition in the excited state.

3. Holographic superfluid with excited states (in the Einstein gravity)

Wang, **Pan***, Lai* and Jing, *PLB* 845, 138134 (2023)

Xu*, Wang*, and **Pan***, *PRD* 110, 046003 (2024)

The action: $$S=\int d^{d+1}x\sqrt{-g}\left\{\frac{1}{2\kappa^2}\left[R+\frac{d(d-1)}{L^2}\right]-\frac{1}{4}F_{\mu\nu}F^{\mu\nu}-|\nabla\psi-iqA\psi|^2-m^2|\psi|^2\right\}$$

In the probe limit, the planar Schwarzschild-AdS black hole:

$$ds^2=-f(r)dt^2+\frac{dr^2}{f(r)}+r^2dx_idx^i \qquad \boxed{f(r)=r^2(1-r_+^d/r^d)/L^2}$$

Turning on the spatial component of the gauge field, we obtain the equations of motion:

$$\boxed{\psi=\psi(r),\quad A_\mu=(A_t(r),0,A_x(r),\ldots)}$$

$$\psi''+\left(\frac{d-1}{r}+\frac{f'}{f}\right)\psi'+\left(\frac{q^2A_t^2}{f^2}-\frac{q^2A_x^2}{r^2f}-\frac{m^2}{f}\right)\psi=0$$

$$A_t''+\frac{d-1}{r}A_t'-\frac{2q^2\psi^2}{f}A_t=0$$

$$A_x''+\left(\frac{d-3}{r}+\frac{f'}{f}\right)A_x'-\frac{2q^2\psi^2}{f}A_x=0$$

Near the AdS boundary, the asymptotic behaviors of the solutions:

current

$$\psi = \frac{\psi_-}{r^{\triangle_-}} + \frac{\psi_+}{r^{\triangle_+}}, \quad A_t = \mu - \frac{\rho}{r^{d-2}}, \quad A_x = S_x - \frac{J_x}{r^{d-2}}$$

$$\triangle_\pm = (d \pm \sqrt{d^2 + 4m^2L^2})/2$$

superfluid velocity

The grand potential in the superfluid phase:

$$\frac{\Omega_S}{V_{d-1}} = -\frac{T\mathcal{S}_{os}}{V_{d-1}} = -\frac{(d-2)}{2}\mu\rho + \frac{(d-2)}{2}S_x J_x - \int_{r_+}^{\infty} q^2 r^{d-3}\psi^2\left(A_x^2 - \frac{r^2 A_t^2}{f}\right)dr$$

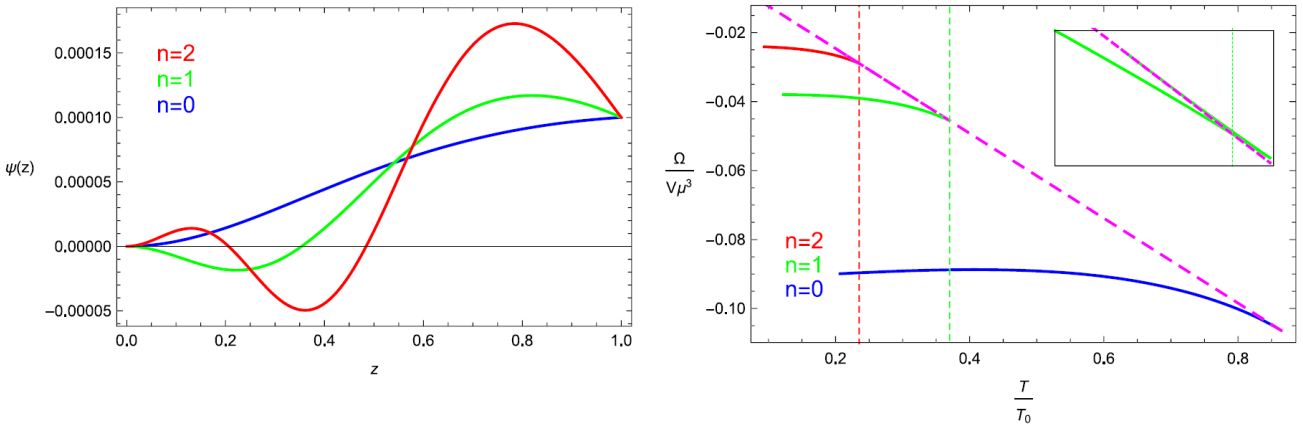

Fig. 1. The scalar field $\psi(z)$ as a function of the radial coordinate z outside the horizon (left) and the grand potential Ω as a function of the temperature T (right) for the fixed mass of the scalar field $m^2L^2 = -2$ and superfluid velocity $S_x/\mu = 0.24$ in the case of $d = 3$. In each panel, the blue, green and red solid lines denote the ground $(n = 0)$, first $(n = 1)$ and second $(n = 2)$ states, respectively. For the right panel, the magenta dotted line corresponds to the normal phase and the vertical line represents the critical temperature (critical chemical potential) of the first-order phase transition.

Condensates of the scalar field

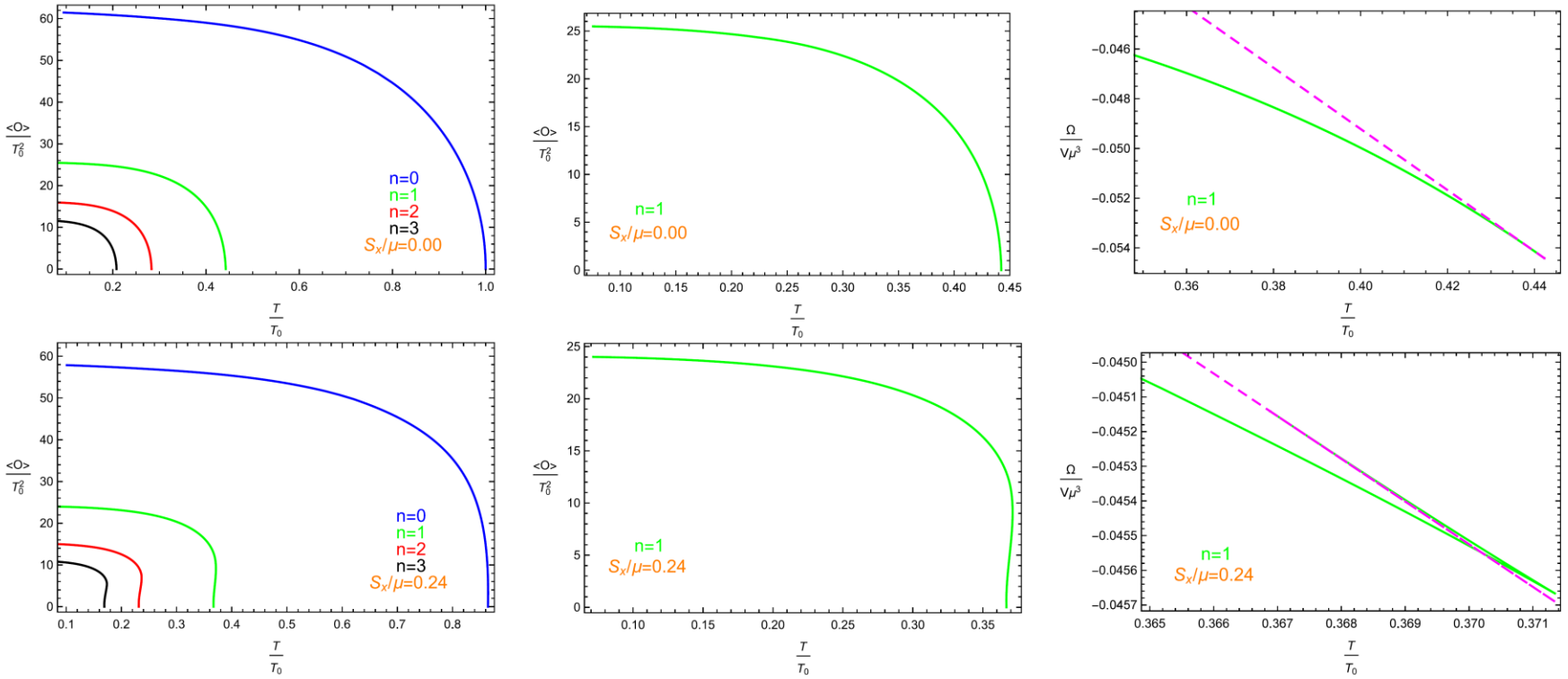

(1) The higher excited state or larger superfluid velocity will make the scalar hair more difficult to be developed.

(2) The superfluid phase transition will change from the second order to the first order when the superfluid velocity increases.

$d = 3$

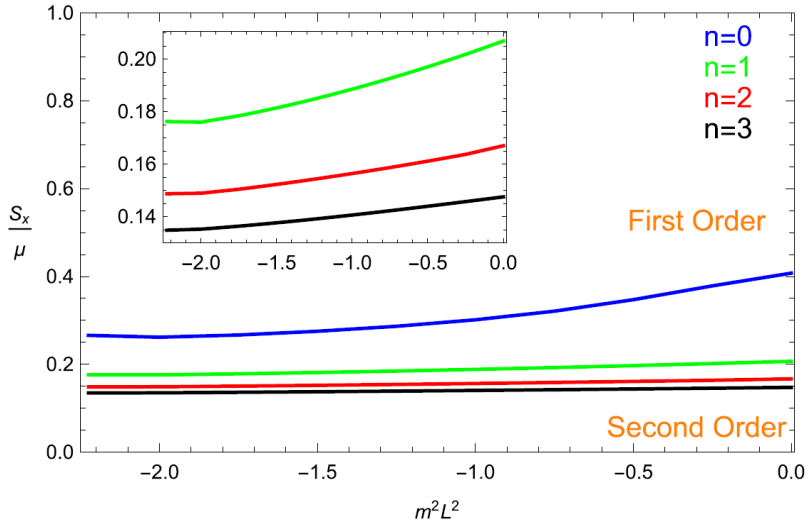

Fig. 3. The translating superfluid velocity S_x/μ from the second to the first order as a function of the scalar mass m^2L^2 for the ground ($n = 0$, blue), first ($n = 1$, green), second ($n = 2$, red) and third ($n = 3$, black) states, respectively.

The higher excited state or smaller mass of the scalar field makes it easier for the emergence of translating point from the second-order transition to the first-order one.

Table 1
The critical chemical potential μ_c with the fixed mass of the scalar field $m^2L^2 = -2$ for different values of S_x/μ from the ground state to the sixth excited state in the case of $d = 3$.

n	0	1	2	3	4	5	6
$S_x/\mu = 0.00$	4.064	9.188	14.357	19.539	24.726	29.916	35.106
$S_x/\mu = 0.24$	4.702	10.977	17.277	23.586	29.900	36.216	42.533
$S_x/\mu = 0.40$	6.074	14.021	21.999	29.987	37.978	45.972	53.968

$$\mu_c \approx \begin{cases} 5.177n + 4.026, & S_x/\mu = 0.00 \\ 6.307n + 4.678, & S_x/\mu = 0.24 \\ 7.984n + 6.047, & S_x/\mu = 0.40 \end{cases}$$

(1) The critical chemical potential becomes evenly spaced for the number of nodes, and the difference of between the consecutive states increases as the superfluid velocity increases.

(2) This conclusion still holds in higher dimensions.

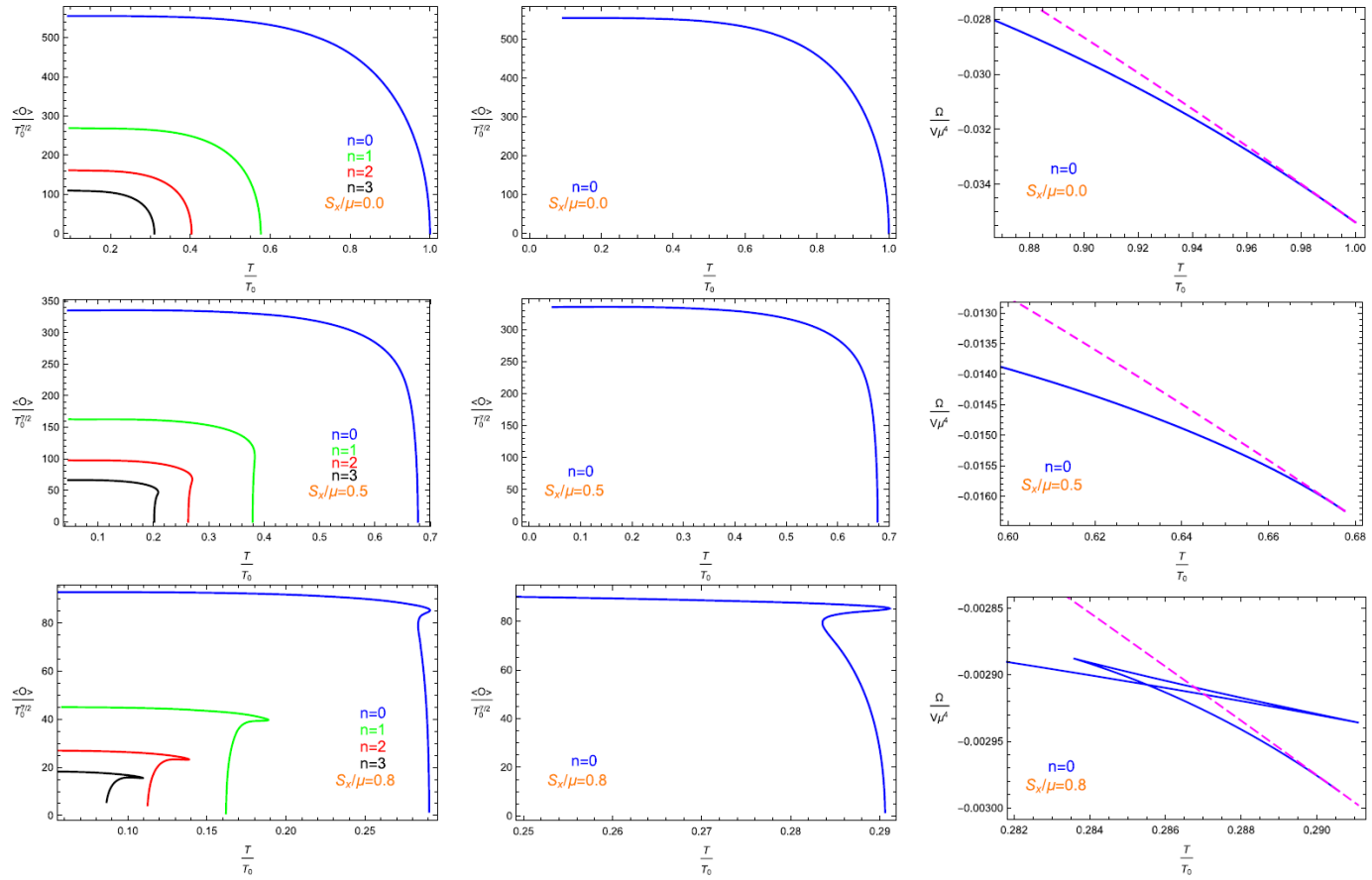

Fig. 4. The condensate and grand potential as a function of the temperature with the fixed mass of the scalar field $m^2L^2 = -7/4$ for different values of S_x/μ from the ground state to the third excited state in the case of $d = 4$. For the left three panels, the four lines in each panel from top to bottom correspond to the ground ($n = 0$), first ($n = 1$), second ($n = 2$) and third ($n = 3$) states, respectively. For the middle three panels, the line in each panel corresponds to the ground state $n = 0$. For the right three panels, the two lines in each panel correspond to the ground state $n = 0$ (blue solid) and the normal phase (magenta dotted) respectively.

The "Cave of Winds" phase structure will disappear but the first-order phase transition occurs for the excited states, which is completely different from the holographic superfluid model with the ground state.

Conductivity

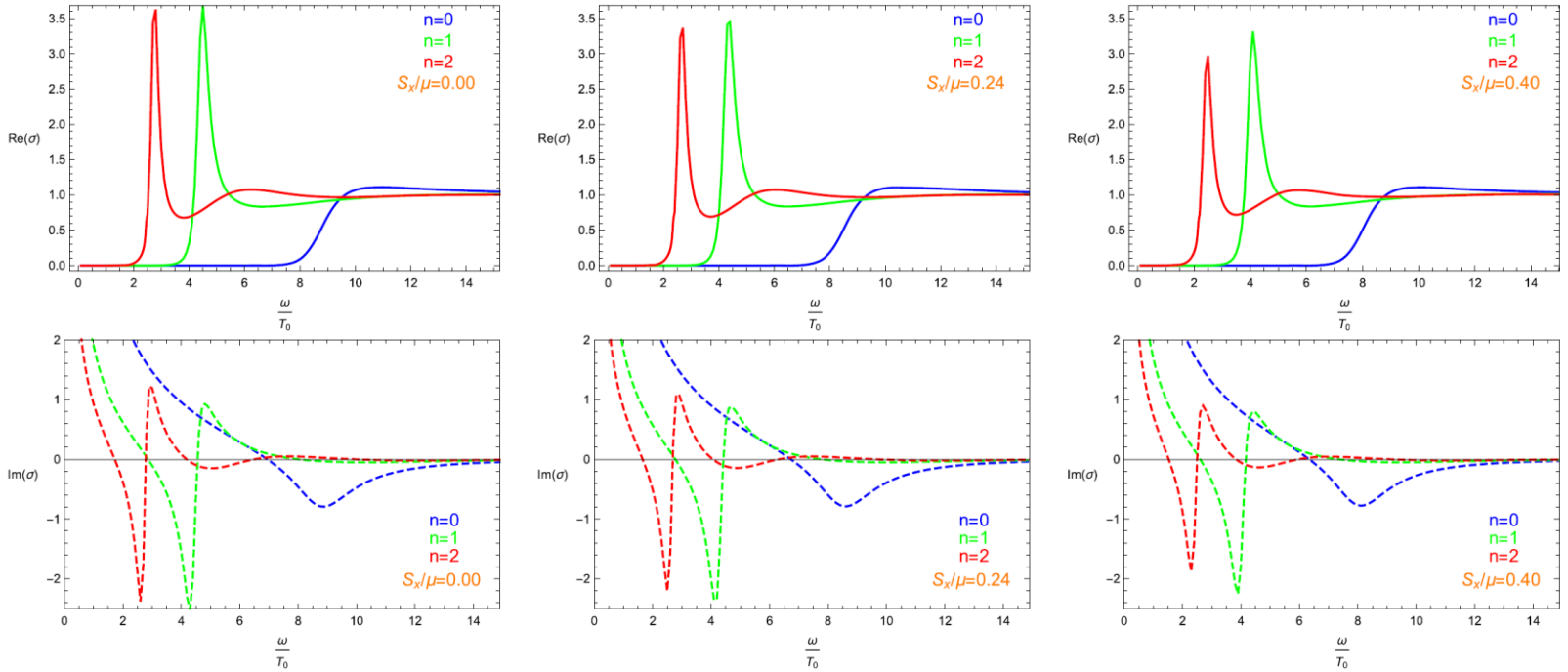

Fig. 5. The conductivity in the holographic superfluid with the fixed mass of the scalar field $m^2L^2 = -2$ for different values of S_x/μ from the ground state to the second excited state where the solid line and dashed line represent the real part $\mathrm{Re}(\sigma)$ and imaginary part $\mathrm{Im}(\sigma)$ of the conductivity. In each panel, the blue, green and red lines denote the ground $(n = 0)$, first $(n = 1)$ and second $(n = 2)$ states, respectively.

There exist additional poles in *Im*[σ(ω)] and delta functions in *Re*[σ(ω)] arising at low temperature for the excited states, and the higher excited state or larger superfluid velocity results in the larger deviation from the expected relation in the gap frequency.

4、Conclusions

- **Holographic superconductors with excited states**

A. We proposed a general analytic technique to investigate its properties, and showed that the excited state has a lower critical temperature than the corresponding ground state.

B. We observed that the holographic entanglement entropy (HEE) and holographic subregion complexity (HSC) provide richer physics in phase transitions and condensation of scalar hair.

- **Holographic superfluid with excited states**

We constructed a novel family of solutions of the holographic superfluid model with the excited states in the probe limit, and obtained the rich phase structure of the system.


Thanks for your attention!